ELSEVIER

Physica D 129 (1999) 15–34

PHYSICA D

Time delay effects on coupled limit cycle oscillators at Hopf bifurcation

D.V. Ramana Reddy, A. Sen *, G.L. Johnston[1]

Institute for Plasma Research, Bhat, Gandhinagar 382428, Gujrat, India

Received 19 October 1998; accepted 5 January 1999
Communicated by Y. Kuramoto

Abstract

We present a detailed study of the effect of time delay on the collective dynamics of coupled limit cycle oscillators at Hopf bifurcation. For a simple model consisting of just two oscillators with a time delayed coupling, the bifurcation diagram obtained by numerical and analytical solutions shows significant changes in the stability boundaries of the amplitude death, phase locked and incoherent regions. A novel result is the occurrence of amplitude death even in the absence of a frequency mismatch between the two oscillators. Similar results are obtained for an array of N oscillators with a delayed mean field coupling and the regions of such amplitude death in the parameter space of the coupling strength and time delay are quantified. Some general analytic results for the $N \to \infty$ (thermodynamic) limit are also obtained and the implications of the time delay effects for physical applications are discussed.

PACS: 05.45.+b; 87.10.+e

Keywords: Coupled oscillators; Time delay; Hopf bifurcation; Amplitude death; Synchronization; Phase locking

1. Introduction

The collective behavior of a large assembly of coupled nonlinear oscillators provides valuable clues for understanding the complex dynamics of systems with many degrees of freedom. This has been one of the major motivations for the recent large scale interest, both experimentally [1] and numerically [2,3], in the study of such simple mathematical models and their application to a wide variety of physical and biological problems. Examples of such applications include interactions of arrays of Josephson junctions [3–5], semiconductor lasers [6,7], charge density waves [8], phase locking of relativistic magnetrons [9], Belousov–Zhabotinskii reactions in coupled Brusselator models [10–13] and neural oscillator models for circadian pacemakers [14]. One of the prominent cooperative phenomena, that was first highlighted by Winfree [15,16] in a simple model of weakly coupled limit cycle oscillators, is that of frequency entrainment or synchronization of the diverse frequencies of the oscillator assembly to a single common frequency [17–21]. This happens in a spontaneous and abrupt fashion once the coupling strength exceeds

* Corresponding author. Tel.: +91-79-2864690; fax: +91-79-2864310; e-mail: abhijit@plasma.ernet.in.
[1] Present address: 12 Billings St., Acton, MA 01720, USA.

0167-2789/99/$ – see front matter
PII: S0167-2789(99)00004-4

a critical threshold. Real life examples of such behavior are abound in nature, e.g. the synchronous flashing of a swarm of fire flies, the chirping of crickets in unison or the electrical synchrony in cardiac cells. When the coupling between the oscillators is comparable to the attraction to their individual limit cycles, other interesting phenomena can occur [22–25] which involve the amplitudes of the individual oscillators. For example, if the coupling is sufficiently strong and the spread in the natural frequencies of the oscillators sufficiently broad, the oscillators can suffer an amplitude quenching or death [26–28]. Such behavior has been observed in experiments of coupled chemical oscillator systems, e.g. coupled Belousov–Zhabotinskii reactions carried out in coupled tank reactors [29]. Other collective phenomena that these coupled oscillator models display include partial synchronization, phase trapping, large amplitude Hopf oscillations and even chaotic behavior [30,31] – all of which have been discussed widely in the literature.

The goal of our present study is to examine the effect of time delay on the collective dynamics of coupled oscillator systems. Time delay is ubiquitous in most physical and biological systems like optical bistable devices [32], electromechanical systems [33], predator–prey models [34], and physiological systems [35,36]. They can arise from finite propagation speeds of signals, for example, or from finite processing times in synapses, finite reaction times in chemical processes and so on. Surprisingly, most past studies on coupled oscillator systems have not considered the effect of time delay. The work of Schuster and Wagner [37], Niebur et al. [38], Nakamura et al. [39] and Kim et al [40], are the only ones, that we are aware of, where they have tried to incorporate time delay effects in the context of the coupled oscillator problem. However, they have restricted themselves to the simplest of models, that of coupled limit cycle oscillators in the weak coupling limit where only the phase information is retained and phenomena like amplitude death cannot occur. Our aim is to extend this study into the strong coupling regime where both phase and amplitude responses need to be retained and to investigate the effect of time delay on the various collective responses of such a model system. To keep the analysis simple, we begin with just two limit cycle oscillators that are coupled with a time delay. For such a model, the bifurcation diagram is easy to obtain both analytically as well as numerically. Furthermore, it allows us a detailed comparison with the past work of Aronson et al. [26] who have analyzed an analogous model but without any time delay in the coupling. After identifying and briefly discussing the results of time delay effects in this simple $N = 2$ model, we next proceed to analyze a large assembly of coupled limit cycle oscillators. For this study, we construct a model which is a generalization of the mean field model of Matthews et al. [30,31] and where the coupling term is suitably modified to introduce time delay. This model is explored in detail by extensive numerical solutions and linear stability analysis around fixed points. The limit of $N \to \infty$ is particularly interesting and permits some explicit analytic results. Our principal focus is on cooperative phenomena like amplitude death and frequency locking and we find that both these states are significantly influenced by time delay effects. One of the surprising and dramatic results is that in the presence of time delay, amplitude death can occur even for zero frequency mismatch between the oscillators (i.e. for identical oscillators). This is in sharp contrast to the situation with no time delay where all previous numerical and analytical works have emphasized the need to have a broad frequency spread for amplitude death to occur. A brief report of this result has been published by us elsewhere [41]. In this paper, we give a more detailed and complete description of this phenomenon. We also report on other newer findings related to time delay induced effects in the collective regimes corresponding to *phase locked* and chaotic states.

The organization of the paper is as follows. In the next section (Section 2), we analyze the model of two limit cycle oscillators that have a time delayed coupling and compare and contrast our results with the previous work of Aronson et al. In Section 3, we describe the more general N coupled oscillator model and present numerical as well as analytic results for the different collective states. This includes the amplitude death region, the phase locked region and the so-called chaotic regime. Some explicit results for the $N \to \infty$ (thermodynamic) limit are also presented. Section 4 provides a summary of our results and a brief discussion on possible future extensions of this work.

2. Two delay coupled oscillators

2.1. Model equations

For the fundamental oscillator unit of our model, we choose the simple limit cycle oscillator described by the equation

$$\dot{Z}_j(t) = (1 + \mathrm{i}\omega_j - |Z_j(t)|^2)Z_j(t), \tag{1}$$

where Z_j is the complex amplitude of the jth oscillator. Each oscillator has a stable limit cycle of unit amplitude $|Z_j| = 1$ with angular frequency ω_j. We consider a simple model in which two of them are coupled linearly to each other as follows,

$$\dot{Z}_1(t) = (1 + \mathrm{i}\omega_1 - |Z_1(t)|^2)Z_1(t) + K[Z_2(t-\tau) - Z_1(t)], \tag{2}$$

$$\dot{Z}_2(t) = (1 + \mathrm{i}\omega_2 - |Z_2(t)|^2)Z_2(t) + K[Z_1(t-\tau) - Z_2(t)], \tag{3}$$

where $K \geq 0$ is the coupling strength and $\tau \geq 0$ is a measure of the time delay. These model equations are a direct generalization of the set of equations studied by Aronson et al. [26] which do not have any time delay. The coupled equations represent the interaction between weakly nonlinear oscillators (that are near a supercritical Hopf bifurcation) and whose coupling strength is comparable to the attraction of the limit cycles. It is important then to retain both the phase and amplitude response of the oscillators. Writing $Z_j = r_j \mathrm{e}^{\mathrm{i}\theta_j}$, Eqs. (2) and (3) can also be expressed in polar form as

$$\dot{r}_1 = r_1(1 - K - r_1^2) + K r_2(t-\tau)\cos[\theta_2(t-\tau) - \theta_1], \tag{4}$$

$$\dot{r}_2 = r_2(1 - K - r_2^2) + K r_1(t-\tau)\cos[\theta_1(t-\tau) - \theta_2], \tag{5}$$

$$\dot{\theta}_1 = \omega_1 + K\frac{r_2(t-\tau)}{r_1}\sin[\theta_2(t-\tau) - \theta_1], \tag{6}$$

$$\dot{\theta}_2 = \omega_2 + K\frac{r_1(t-\tau)}{r_2}\sin[\theta_1(t-\tau) - \theta_2]. \tag{7}$$

For $\tau = 0$, the work of Aronson et al. [26] shows that the nonlinear Eqs. (4)–(7) have a variety of stationary and nonstationary solutions which depend on the strength of the coupling parameter K and the frequency mismatch between the oscillators $\Delta = |\omega_1 - \omega_2|$. For extremely weak coupling ($K \to 0$) and large Δ, the oscillators behave independently and the long term behavior is a nonstationary incoherent state in which the relative phase of the two oscillators moves through all phases. Such a state is also called a *phase drift* state. With increasing coupling strength, two important classes of stationary solutions are possible. One of them is *amplitude death* in which the oscillators pull each other off their cycles and collapse into the origin ($r_1 = r_2 = 0$) as $t \to \infty$. The other collective state is called *frequency locking* or *mutual entrainment* in which the two oscillators synchronize to a common frequency and the time asymptotic state is one of coherent or collective oscillation. The distribution of these solutions can be neatly represented in a phase diagram (bifurcation diagram) in the $\Delta - K$ space. Fig. 1, reproduced from the work of Aronson et al. [26] summarizes the above discussion. Region I represents the amplitude death region, region II marks the phase locked state and region III is the phase drift regime. We now analyze Eqs. (4)–(7) for finite values of τ and examine the effect of τ on the conditions for the onset of these states and changes if any in the basic properties of these states. In the following subsections, we discuss the results for the amplitude death and phase locked solutions.

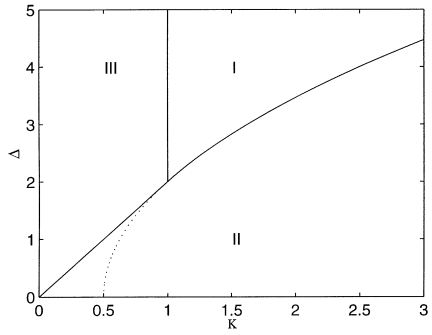

Fig. 1. Bifurcation diagram of Aronson et al. of two coupled oscillators without time delay in the plane of coupling strength (K) and the frequency mismatch (Δ). Region I, bounded by the curves $K = 1$ and $K = (1 + \Delta^2/4)/2$, represents the oscillator death region. Region II, bounded by $K = \Delta/2$ (when $\Delta < 2$) and $K = (1 + \Delta^2/4)/2$ (when $\Delta > 2$), represents the frequency locked state. Region III represents the incoherent or drift solutions. All the three regions meet at a degenerate point $(K, \Delta) = (1, 2)$.

2.2. Amplitude death

As is clear from Eqs. (2) and (3), the origin $Z_j = 0$, $j = 1$ and 2, is always a fixed point of the system. The question to consider is whether this is a stable fixed point in which case all amplitudes of the oscillators would collapse into the origin as $t \to \infty$. In the absence of time delay, this state occurs in the region $K > 1$ for $\Delta > 2$. To determine the onset conditions of this state in the presence of time delay ($\tau \neq 0$), we linearize Eqs. (2) and (3) around $Z_j = 0$ to obtain the characteristic equation,

$$\det(A - \lambda I) = 0, \tag{8}$$

where A, the linearized matrix of Eqs. (2) and (3), is given by

$$A = \begin{bmatrix} a + \mathrm{i}\omega_1 & K\mathrm{e}^{-\lambda\tau} \\ K\mathrm{e}^{-\lambda\tau} & a + \mathrm{i}\omega_2 \end{bmatrix}, \tag{9}$$

I is the identity matrix, $a = 1 - K$ and the perturbations are assumed to have a time dependence proportional to $\mathrm{e}^{\lambda t}$. Eq. (8) can be written in the form

$$(a - \lambda + \mathrm{i}\omega_1)(a - \lambda + \mathrm{i}\omega_2) - K^2\,\mathrm{e}^{-2\lambda\tau} = 0 \tag{10}$$

or

$$\lambda^2 - 2(a + \mathrm{i}\bar{\omega})\lambda + (b_1 + \mathrm{i}b_2) + c\mathrm{e}^{-2\lambda\tau} = 0, \tag{11}$$

where $b_1 = a^2 - \bar{\omega}^2 + \Delta^2/4$, $b_2 = 2a\bar{\omega}$, $\Delta = |\omega_1 - \omega_2|$, $\bar{\omega} = (\omega_1 + \omega_2)/2$ and $c = -K^2$. This is a transcendental equation having an infinite number of roots and we wish to study the movement of the eigenvalues in the parametric plane of (K, Δ) and (K, τ). Setting $\lambda = \alpha + \mathrm{i}\beta$, where α and β are real, the amplitude death region corresponds to the region in which $\alpha < 0$. The marginal stability curves or the critical curves are thus obtained by requiring that $\alpha = 0$, i.e. $\lambda = \mathrm{i}\beta$. Substituting in Eq. (10), the equations defining the critical curves are thus given by

$$(\beta - \bar{\omega})^2 - \frac{\Delta^2}{4} - a^2 + K^2\cos(2\beta\tau) = 0, \tag{12}$$

$$2a(\beta - \bar{\omega}) - K^2\sin(2\beta\tau) = 0. \tag{13}$$

We first briefly describe the case of $\tau = 0$, in order to appreciate the changes brought about by finite time delay. Setting $\tau = 0$ in Eq. (13), we obtain the conditions $K = 1$ and $\beta = \bar{\omega}$. Substituting for β in Eq. (12), we obtain

$K = \gamma(\Delta) = (1/2)(1 + \Delta^2/4)$. So the critical curves in this case are $K = 1$ and $K = \gamma(\Delta)$ in agreement with the work of Aronson et al. [26] and as illustrated in Fig. 1. It is appropriate to distinguish between two regions in the (K, Δ) space, namely (i) $\Delta > 2$ and (ii) $\Delta < 2$. When $\Delta > 2$, the stable region of the origin (amplitude death region) is bounded by $K = 1$ and $K = \gamma(\Delta)$. The eigenvalues in this particular case can be written down (from Eq. (11)) as $\lambda = 1 - K \pm \sqrt{K^2 - \Delta^2/4} \pm i\bar{\omega}$. On the boundary $K = 1$, the origin loses stability in a Hopf bifurcation. Two pairs of eigenvalues cross into the right half plane. On the boundary $K = \gamma(\Delta)$, a pair of eigenvalues crosses into the right hand side (RHS) of the complex eigenvalue plane, giving rise to a single frequency, which corresponds to the phase locked state of the system. In the second case, when $\Delta < 2$, there is no amplitude death. However, the critical curves give a boundary on which an unstable fixed point is born as one moves to the left of $K = \gamma(\Delta)$ curve. Note also that the boundaries of the three regions meet in a highly degenerate manner in the single point $K = 1$, $\Delta = 2$. Another distinguishing feature of the $\tau = 0$ case is that the critical curves are independent of the mean frequency $\bar{\omega}$. In fact, one can set $\bar{\omega} = 0$ (which is equivalent to transforming to a frame rotating at the mean frequency) and carry out the same analysis without any loss of generality. This property follows from the original symmetry of the coupled equations.

When $\tau \neq 0$, this symmetry is lost and the critical curves are no longer independent of $\bar{\omega}$ as seen from Eqs. (12) and (13). In comparing the phase diagrams of the $\tau \neq 0$ case with that of the Aronson et al. [26] diagram, we therefore need to always mention the specific value of the mean frequency parameter. We now briefly describe our numerical procedure for solving Eqs. (12) and (13) in order to plot graphically the critical curves in the (K, Δ) space. To eliminate β between the two equations, it is more convenient to write the equations in the following parametric form,

$$F = \frac{(\beta - \bar{\omega})}{\sin(2\beta\tau)}, \tag{14}$$

$$K \equiv K_{\pm} = -F \pm \sqrt{F^2 + 2F}, \tag{15}$$

$$\Delta^2 = -4a^2 + 4(\beta - \bar{\omega})^2 + 4K^2 \cos(2\beta\tau), \tag{16}$$

where Eq. (15) corresponds to the two roots of K for the quadratic equation (13). Eqs. (14)–(16) represent two sets of curves arising due to the $\pm$ signs. Let us denote the set of curves arising due to the '+' sign by $S_+ \equiv S_+(K_+, \Delta)$ and the curves due to the '−' sign by $S_- \equiv S_-(K_-, \Delta)$. The curves S_+ and S_- are obtained by choosing an interval of β and correspondingly evaluating K and Δ and thus eliminating β. The function F has singularities at $\beta = \beta_n = n\pi/2\tau$, where n is an integer. Each interval $I = (\beta_n, \beta_{n+1})$ provides a part of the phase curves in (K, Δ) plane. In the (K, Δ) space, the curves S_- exist between $K = 1$ and $K = 2$ and the curves S_+ exist outside this region in the intervals $1/2 < K < 1$ and $K > 2$. And at higher values of τ, S_- produces curves which could intersect. For small values of the parameter τ close to 0, the amplitude death region is bounded by the curve S_- when $K < 1$ and S_+ when $K > 1$. At higher value of τ, the boundary of the death region falls below $K = 1$ in which region the boundary is specified by the curves S_+. The transcendental Eqs. (14)–(16) must be studied for each parametric value of τ, since the curves in (K, Δ) space become more complicated as the parameter τ is increased.

We now present our results of the amplitude death region for $\bar{\omega} = 10$ for various values of τ as obtained by the numerical prescription described above. From the series of diagrams in Fig. 2, we notice that with the introduction of finite τ, the point $(K = 1, \Delta = 2)$ no longer has a degenerate character and the critical curves begin separating and distorting in a continuous manner. The amplitude death region grows in size as the value of τ is increased from 0 and the curve S_+ defined by the interval of $\beta \in (0, \bar{\omega})$ starts bending down below the $\Delta = 2\sqrt{2K - 1}$ curve towards the $\Delta = 0$ axis. For a critical value of $\tau = \tau_c$, it touches the $\Delta = 0$ axis and the region of death on the axis lies between the two points of intersection K_1 and K_2 of S_+ with $\Delta = 0$. This death region has a finite width $K_2 - K_1$ for a range of values of the delay parameter τ. This phenomenon of death of identical oscillators is a novel

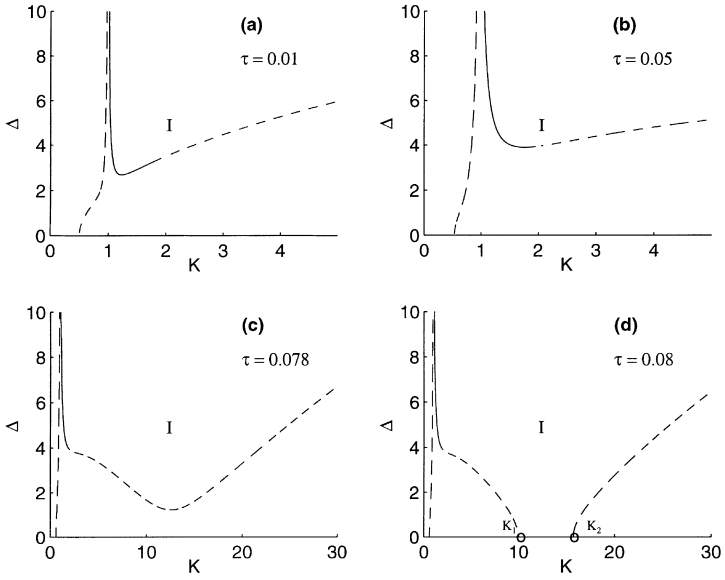

Fig. 2. The effect of time delay on the boundary of the amplitude death region of two coupled oscillators. The critical curves are plotted from Eqs. (14)–(16) for $\bar{\omega} = 10$. Region I represents the amplitude death region. For small values of τ, the degenerate point $(K, \Delta) = (1, 2)$ disappears and the death region is bounded by the curves S_- (solid lines) and S_+ (dashed lines) as defined in the text. As the delay parameter τ is increased, the bounding curves get deformed continuously.

result purely induced by the temporal delay in the coupling of the oscillators. This behavior presents for a range of τ after which the bifurcation curve lifts up from the $\Delta = 0$ line and starts moving upward.

To quantitatively study this region of amplitude death for identical oscillators, we take a more detailed look at the trajectory of the two bounding points K_1 and K_2 in the parametric space of (K, τ) for $\Delta = 0$. Let this trajectory be called $\tau_b(K)$ for which we require that all the eigenvalues of the original transcendental equation lie in the left half plane of the complex eigenvalue plane when $\tau > \tau_c$. To identify such a curve from all the permissible multiple critical curves in the parametric space (K, τ), it is simpler to start with the original Eq. (10) and set $\omega_1 = \omega_2 = \omega_0$ in it. The eigenvalue equation now simplifies to

$$\lambda = 1 - K + \mathrm{i}\omega_0 \pm K\mathrm{e}^{-\lambda\tau}. \tag{17}$$

Let $\lambda = \alpha + \mathrm{i}\beta$, where α and β are real. We assume without loss of generality that $\beta \geq 0$. In order to obtain the critical curves, we set $\alpha = 0$ and consider both the equations arising out of '+' and '−' signs in Eq. (17). After some straightforward algebra, involving the choice of the correct signs in the inversion of the cosine function, we obtain the following two sets of critical curves,

$$\tau_1 \equiv \tau_1(n, K) = \frac{n\pi + \cos^{-1}(1 - 1/K)}{\omega - \sqrt{2K - 1}}, \tag{18}$$

$$\tau_2 \equiv \tau_2(n, K) = \frac{(n+1)\pi - \cos^{-1}(1 - 1/K)}{\omega + \sqrt{2K - 1}}, \tag{19}$$

where $n = 0, 1, \ldots, \infty$. We further need to know the nature of the transition of pairs of eigenvalues as it crosses these curves. For this, it is necessary to evaluate $\mathrm{d}\alpha/\mathrm{d}\tau$ on each of these curves and examine its sign. Setting

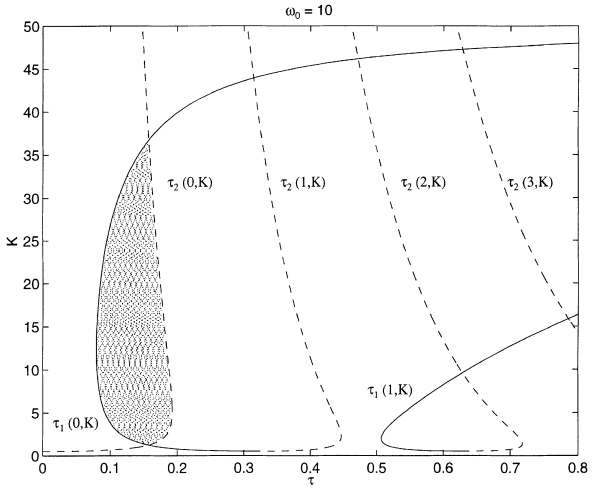

Fig. 3. The death island. The amplitude death region for identical oscillators with a common frequency of $\bar{\omega} \equiv \omega_0 = 10$ in (K, τ) space. The island boundaries are defined by $\tau_1(0, K)$ and $\tau_2(0, K)$. No other regions of amplitude death region exist for this value of ω_0.

$\lambda = \alpha + \mathrm{i}\beta$ in Eq. (17) and differentiating with respect to τ, it is straightforward to get

$$\left.\frac{\mathrm{d}\alpha}{\mathrm{d}\tau}\right|_{\alpha=0} = c_1\beta(\beta - \omega_0) = \begin{cases} c_1\sqrt{2K-1}(\omega_0 + \sqrt{2K-1}), & \text{if } \beta = \beta_+, \\ -c_1\sqrt{2K-1}(\omega_0 - \sqrt{2K-1}), & \text{if } \beta = \beta_-, \end{cases} \tag{20}$$

where $c_1 = [(1 \pm K\tau)^2 + (K\tau\sin(\beta\tau))^2]^{-1}$, which is a real positive constant and $\beta \equiv \beta_\pm = \omega_0 \pm \sqrt{2K-1}$. From the above equation it is easily seen that

$$\left.\frac{\mathrm{d}\alpha}{\mathrm{d}\tau}\right|_{\alpha=0} \begin{cases} < 0 & \text{on } \tau_1 \text{ if } K < f(\omega_0), \\ > 0 & \text{on } \tau_1 \text{ if } K > f(\omega_0), \\ > 0 & \text{on } \tau_2, \end{cases} \tag{21}$$

where $f(\omega_0) = (1 + \omega_0^2)/2$. Thus on a τ_1 curve, a pair of eigenvalues transits to the left half plane, provided the coupling strength is smaller than $f(\omega_0)$ and to the right side if the coupling strength is greater than $f(\omega_0)$. On a τ_2 branch of the critical curves, however, a pair of eigenvalues always crosses into the right half plane of the complex plane. Thus, for a finite region of amplitude death to exist in the $K - \tau$ plane, it needs to be bounded by appropriate branches of the τ_1 and τ_2 curves and condition $K < f(\omega_0)$ should hold. For $K > f(\omega_0)$, there would be no amplitude death region at all.

In Fig. 3, we illustrate the above arguments more graphically by plotting the critical curves $\tau_1(n, K)$ (solid lines) and $\tau_2(n, K)$ (dashed lines) for the first few value of n and for $\bar{\omega} = 10$ in the $K - \tau$ space. It is possible to identify $\tau_1(0, K)$ as $\tau_\mathrm{b}(K)$. This curve forms the first boundary of the amplitude death region of identical oscillators in (K, τ) space. The stability of the origin can be lost when a pair of eigenvalues makes a transition to the right half plane, which in the present case will occur on $\tau_2(0, K)$ (as can be verified from Eq. (21)). So the region enclosed by the intersection of $\tau_1(0, K)$ and $\tau_2(0, K)$ forms a region of amplitude death in the $K - \tau$ space, which we label as a *death island*. Physically, such an island represents a region in phase space where for a given value of ω and at a fixed K, we move (by varying τ) from an unstable region (corresponding to phase locked states) into a stable region as we cross the left boundary of the island to emerge again into an unstable region as we cross the right boundary of the island. Is it possible to have more than one island for a given value of ω_0? To answer this question, we see from Fig. 3, that the next curve along the τ axis is $\tau_2(1, K)$ on which another pair of eigenvalues will make a transition

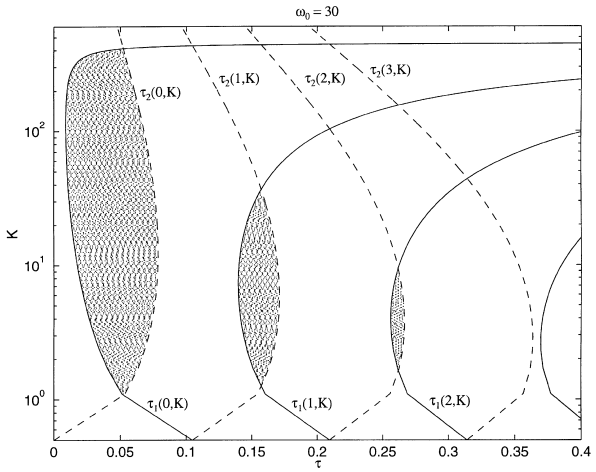

Fig. 4. The existence of multiple death islands. In the (τ, K) space the amplitude death region is multiply connected (i.e. higher order death islands exist) for higher values of ω_0. The figure shows that for $\omega_0 = 30$, there are three death islands which are defined by the set of curves $\tau_{1,2}(m, K)$ where $m = 0, 1, 2$.

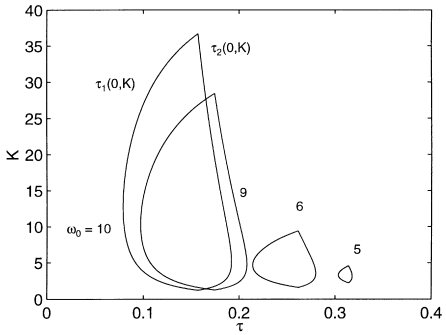

Fig. 5. Dependence of the size of the death island on the common intrinsic frequency, ω_0. Below a certain threshold, which is given by the condition of intersection of the curves $\tau_1(0, K)$ and $\tau_2(0, K)$, the amplitude death region disappears. This value, found numerically, is 4.812.

to the right half plane. Thus, when one gets to $\tau_1(1, K)$, which is the next in the sequence and on which a pair of eigenvalues crosses to the left half plane, there is still a pair left in the right half plane. Thus, the region between $\tau_1(1, K)$ and $\tau_2(2, K)$ does not constitute a death island. In general, the frequency of τ_2 curves is higher than τ_1, i.e.,

$$\delta\tau_2(n, K) < \delta\tau_1(n, K), \tag{22}$$

where $\delta\tau_1(n, K) = \tau_1(n + 1, K) - \tau_1(n, K)$ and $\delta\tau_2(n, K) = \tau_2(n + 1, K) - \tau_2(n, K)$. Thus, the death island region is usually singly connected and there are no higher order islands. However, the ordering of the curves depends on the magnitude of ω_0. In the present case, we do not see any multiple islands in the range $4.812 \leq \omega \leq 14.438$. For $\omega_0 > 14.438$, we do see the appearance of higher order islands as shown in Fig. 4 for $\omega_0 = 30$. The size of the primary death island is found to be a function of ω_0 and as we shall see in the next section, it also depends on N, the number of coupled oscillators. Fig. 5 displays the island sizes for different values of ω_0. The size of the island decreases with decreasing frequency and vanishes below a certain threshold.

All the above features of the amplitude death phenomenon have also been confirmed by a direct numerical solution of the coupled oscillator equations and excellent agreement with the analytic results have been found.

2.3. Frequency locking

The frequency (or phase) locked solutions of the system of Eqs. (4)–(7) are characterized by the property that the relative phase of the two oscillators is a constant. The phase locked state can be described by the ansatz $\theta_{1,2}(t) = \Omega t \mp \alpha/2$, where α, the phase difference between the two oscillators, and Ω, the common frequency of the two oscillators are real constants. Substitution of this ansatz in Eqs. (6) and (7) further shows that the amplitudes of the limit cycles remain constant in this case. Thus, the phase locked solutions can be described by the representation, $(r_1(t), r_2(t), \theta_1(t), \theta_2(t)) = (R_1, R_2, \Omega t - \alpha/2, \Omega t + \alpha/2)$, where $R_{1,2}$ are constants. Substituting such a form in Eqs. (4)–(7), we obtain the following set of four equations from which the values of R_1, R_2, Ω and α can be evaluated,

$$(1 - K - R_1^2)R_1 + K R_2 \cos(\alpha - \Omega\tau) = 0, \tag{23}$$

$$(1 - K - R_2^2)R_2 + K R_1 \cos(\alpha + \Omega\tau) = 0, \tag{24}$$

$$\Omega = \omega_1 + K\frac{R_2}{R_1}\sin(\alpha - \Omega\tau), \tag{25}$$

$$\Omega = \omega_2 - K\frac{R_1}{R_2}\sin(\alpha + \Omega\tau). \tag{26}$$

These equations can also be rearranged in the following form which is slightly more convenient for numerical solutions,

$$R_1^2 = 1 - K + K f_1 \cos(\alpha - \Omega\tau), \tag{27}$$

$$R_2^2 = 1 - K + K f_2 \cos(\alpha + \Omega\tau), \tag{28}$$

$$\alpha = \sin^{-1}\sqrt{\sin^2(\Omega\tau) - \frac{(\Omega - \omega_1)(\Omega - \omega_2)}{K^2}}, \tag{29}$$

$$R_2^2 = f_1^2 R_1^2, \tag{30}$$

where $f_1 = (\Omega - \omega_1)/(K\sin(\alpha - \Omega\tau))$ and $f_2 = -(\Omega - \omega_2)/(K\sin(\alpha + \Omega\tau))$. This is a set of transcendental equations whose solutions describe the phase locked equilibria. We again first briefly discuss the $\tau = 0$ case. Putting $\tau = 0$ in Eqs. (27) and (28), we see that there are two possible equilibrium solutions which are given by (i) $R_1^2 = R_2^2 = \rho^2$ which is called the symmetric equilibrium, and (ii) $R_1^2 + R_2^2 = 1 - K$, the asymmetric case. Both these equilibria have been studied in detail by Aronson et al. [26]. The symmetric phase locked equilibria are given by $\rho_\pm^2 = 1 - K \pm \sqrt{K^2 - \Delta^2/4}$, $\Omega = (\omega_1 + \omega_2)/2$ and $\alpha_\pm$, where $\alpha_+ = \sin^{-1}(\Delta/2K)$, and $\alpha_- = \pi - \sin^{-1}(\Delta/2K)$. Of these two symmetric equilibria, the set given by $(\rho_+^2, \Omega, \alpha_+)$ is found to be stable, whereas the solution $(\rho_-^2, \Omega, \alpha_-)$ is unstable. The asymmetric phase locked solutions turn out to be unstable. Thus, for $\tau = 0$, the only stable equilibrium is the one where the two oscillators are synchronized to the mean frequency and have identical amplitudes. Note that the amplitudes are lowered from the unity value of the uncoupled case by the amount $K - \sqrt{K^2 - \Delta^2/4}$.

With finite time delay ($\tau \neq 0$) there is a richer fare of equilibria. This is evident from the full set of transcendental Eqs. (27)–(30) which permit a large number of solutions. Although it is difficult to obtain analytic forms for these

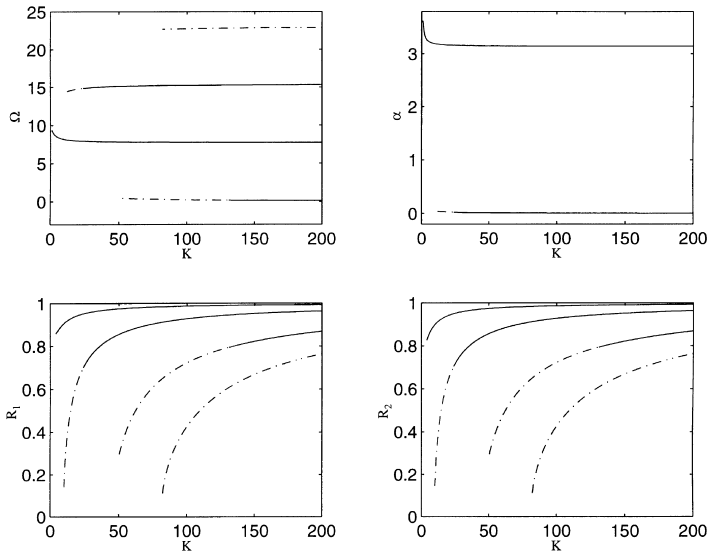

Fig. 6. The phase locked solutions. The common frequency Ω, the phase difference α and the amplitudes of the individual oscillators plotted as a function of the coupling strength, K for $\tau = 0.4084$, $\Delta = 1$, and $\bar{\omega} = 10$. The oscillators have the phase difference α, either around 0 (i.e. in-phase synchronization) or around π (anti-synchronization). The unstable portions of the solutions are plotted as dashed lines.

solutions, it is easy to track these solutions numerically. We have carried out such an analysis and our results for $\tau = 0.4084$ are displayed in Fig. 6. The number of these coherent states increases as a function of K and τ. We have also studied the stability of these states by carrying out a linear perturbation analysis of Eqs. (4)–(7) around the phase locked solutions. The algebraic details of this analysis are given in Appendix A. Numerical solution of the stability conditions shows that all these higher frequency states are stable (except for small bands of unstable regions which are indicated by dashed curves in Fig. 6). Thus, these higher frequency states are genuine collective states of the system that are physically accessible. It should be mentioned that similar collective states were also observed in the delay coupled *phase only* model studied by Schuster et al. [37]. One difference between those results and our amplitude inclusive model is that the frequencies of our model are slightly lower due to amplitude effects. When the phase locked amplitudes of the two oscillators are equal or if their ratio is close to unity, the effect of the amplitude on the magnitude of the phase locked frequencies ceases.

We end this analysis of the $N = 2$ model with a short description of the typical phase diagram for finite time delays. Such a diagram is shown in Fig. 7 for $\tau = 0.4084$, which reveals a much richer structure in comparison to the Fig. 1 of Aronson et al. [26]. Note that one no longer has the clean separation of the Bar-Eli region, the phase locked region and the phase drift region into three disjoint regions that converge at a single degenerate point. Instead, the phase locked region now always surrounds the Bar-Eli region and the single degenerate point is replaced by a series of X points resulting from the braided structure of the phase locked region in the vertical direction. The dotted curve (obtained numerically) marks the separation of the phase locked and the incoherent regions. This curve also represents the birth of two fixed points of the system, one stable and the other unstable. These branches can be seen in Fig. 8 (a), where the phase locked amplitudes are plotted at $\Delta = 2$. The dashed curves are the unstable branches and the solid curves, stable branches. At large values of K, other bifurcation curves appear in the phase locked region indicating the appearance of higher frequency states [37]. Figs. 8(b,c) show, respectively, the phase locked solutions for $\Delta = 7$ as K is varied and for $K = 1$ as Δ is increased. It should be noted that the basic nature of the transitions, namely a supercritical Hopf bifurcation, is preserved in the presence of time delay. Fig. 8(b), a typical example, illustrates this clearly.

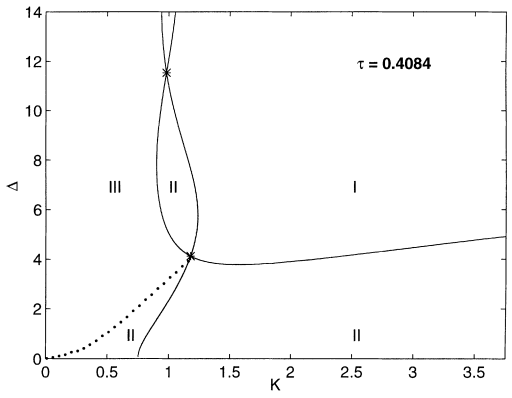

Fig. 7. The bifurcation diagram in the (K, Δ) space for $\tau = 0.4084$ and $\bar{\omega} = 10$. The region marked I is the amplitude death region, II corresponds to the phase locked solutions, and the region III is the phase drift or incoherent region. The dotted curve which separates the phase locked region from the incoherent region is obtained by numerical integration of the original equations. Notice that the degenerate points (marked by stars) have reappeared for this value of the delay parameter τ. At higher values of K, other bifurcation curves appear, indicating higher order frequency states as shown in Fig. 6.

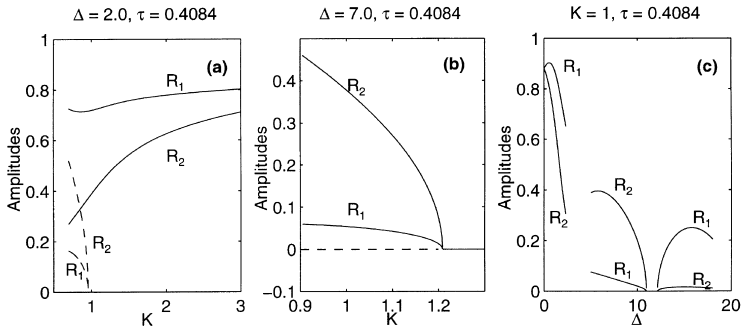

Fig. 8. The amplitude curves R_1 and R_2 of the phase locked solutions of the two oscillators plotted in three different regions. R_1 corresponds to the amplitude of the oscillator with the smaller of the intrinsic frequencies and R_2 that of the larger of the two. (a) At $\Delta = 2$, the stable branches (solid curves) continue to exist, whereas the unstable (dashed curves) of the two oscillators merge with the origin as K is increased. (b) The amplitudes of the oscillators in one of the 'closed loops' in the bifurcation diagram (previous figure) at $\Delta = 7$. The origin is unstable (dashed line) in the region where the periodic orbits are stable and stable outside this region, illustrating the supercritical Hopf bifurcation and (c) shows the phase locked solutions as one moves along the line $K = 1$. In the first gap, there are phase drift solutions and in the second gap, amplitude death solutions.

3. Assembly of N delay coupled oscillators

3.1. Model equations

In this section, we study the interaction of a large number of limit cycle oscillators that are globally coupled with a linear time delayed coupling. To describe such a system, we introduce the following set of model equations,

$$\dot{Z}_j(t) = (1 + \mathrm{i}\omega_j - |Z_j(t)|^2)Z_j(t) + \frac{K'}{N}\sum_{k=1}^{N}[Z_k(t-\tau) - Z_j(t)] - \frac{K'}{N}[Z_k(t-\tau) - Z_j(t)], \tag{31}$$

where $j = 1, \ldots, N$, $K' = 2K$ is the coupling strength and τ is the delay time. The last term on the RHS has been introduced to remove the self-coupling term. The model is a straightforward generalization of the mean field

model studied extensively by Ermentrout [27], Mirollo and Strogatz [28], and others [22] and reduces exactly to their model for $\tau = 0$. Mirollo and Strogatz [28] have provided rigorous analytical and numerical conditions for amplitude death in such a mean field model system. Their conclusions, in general, are similar to the case of $N = 2$, namely, that one needs a sufficiently large variance in frequencies for death to occur and K has to be sufficiently large. In a short while, we will discuss our findings for the time delayed model in the light of their results.

As is customary in mean field models, we can also define a centroid or 'order parameter' of the form

$$\bar{Z} = R\mathrm{e}^{\mathrm{i}\phi} = \frac{1}{N}\sum_{j=1}^{N} Z_j(t), \tag{32}$$

where R and ϕ denote the amplitude and phase of the centroid. The order parameter is a useful quantity in the large N model, since its behavior provides qualitative and quantitative clues about the collective and nonstationary states of the system, e.g. $R = 0$ (in the large time limit) is indicative of an incoherent state, whereas $R = 1$ marks a 'phase locked' state. As has been noted by Matthews and Strogatz [30,31], the time behavior of R can also characterize chaotic states and other nonstationary states like large amplitude Hopf oscillations. We will also examine the behavior of this parameter in certain cases to track the effects of the time delay parameter on the collective dynamics of the large N system. In terms of the order parameter defined above, the model equations can be written as follows,

$$\dot{Z}_j(t) = (1 - K'd + \mathrm{i}\omega_j - |Z_j(t)|^2)Z_j(t) + K'\bar{Z}(t-\tau) - \frac{K'}{N}Z_j(t-\tau), \tag{33}$$

where $d = 1 - 1/N$. To study the stability of the origin, we once again carry out a linear perturbation analysis of Eq. (31) with the perturbation varying as $\mathrm{e}^{\lambda t}$. The linearized matrix of Eq. (31) is given by

$$B = \begin{bmatrix} l_1 & f & \cdots & f \\ f & l_2 & \cdots & f \\ \vdots & \vdots & \ddots & \vdots \\ f & f & \cdots & l_N \end{bmatrix}, \tag{34}$$

where $l_n = 1 - K'd + \mathrm{i}\omega_n$, $f = (K'/N)\mathrm{e}^{-\lambda\tau}$. That is

$$B_{ij} = \begin{cases} 1 - K'd + \mathrm{i}\omega_j, & \text{if } i = j, \\ \frac{K'}{N}\mathrm{e}^{-\lambda\tau}, & \text{if } i \neq j. \end{cases}$$

It is more convenient to cast the eigenvalue problem in terms of another matrix C, where we define $C = B + (K'd - 1)I$ (with I being the identity matrix). If μ is the eigenvalue of C, then it is related to λ by the relation $\mu = \lambda + (K'd - 1)$. The matrix C is given by

$$C_{mn} = \begin{cases} \mathrm{i}\omega_m, & \text{if } m = n, \\ f, & \text{if } m \neq n. \end{cases} \tag{35}$$

The eigenvalues μ are obtained by solving $\det(C - \mu I) = 0$, i.e.,

$$\det \begin{bmatrix} \mathrm{i}\omega_1 - \mu & f & \cdots & f \\ f & \mathrm{i}\omega_2 - \mu & \cdots & f \\ \vdots & \vdots & \ddots & \vdots \\ f & f & \cdots & \mathrm{i}\omega_N - \mu \end{bmatrix} = 0. \tag{36}$$

This eigenvalue equation can be compactly expressed as a product of two factors,

$$\left[\prod_{k=1}^{N}(\mathrm{i}\omega_k - \mu - f)\right]\left[1 + f\sum_{j=1}^{N}\frac{1}{\mathrm{i}\omega_j - \mu - f}\right] = 0. \tag{37}$$

As pointed out by Matthews and Strogatz [30,31], the first factor represents the continuous spectrum of the system, whereas the second factor gives us the discrete spectrum. In general, it is not possible to solve the characteristic equation (37) analytically and for large N, the numerical tracking of all the eigenvalues is also an arduous task. There are two interesting limits however, in which the analysis gets considerably simplified. If the N oscillators have identical frequencies, then it is possible to obtain exact algebraic relations for the critical curves marking the amplitude death region. This is of considerable interest to us in view of the novel result of the $N = 2$ model, which showed amplitude death for $\Delta = 0$. The interesting question to ask is, whether such a phenomenon exists for the arbitrary N case. We will study this question in the next subsection. Another interesting limit is the $N \to \infty$ limit, often called the thermodynamic limit. It is once again possible to obtain some exact analytic results in this limit regarding the behavior of the critical curves in the bifurcation diagram. We will carry out this analysis in Section 3.3. As shown by Mirollo and Strogatz [28] (for the $\tau = 0$ case), the infinite system results are of practical interest since they provide a fairly accurate picture of amplitude death for the large but finite system. A similar conclusion holds for the time delay case as well, as we find out by comparing the analytic results of the thermodynamic limit with numerical solutions for a large number of oscillators. In the final subsection, we look at the time behavior of the order parameter in the various collective regimes and discuss its dependence on the time delay factor. We also briefly discuss the region of nonstationary solutions (chaos, Hopf oscillations etc.) that was first pointed out by Matthews and Strogatz [30,31] for the $\tau = 0$ case.

3.2. Amplitude death of identical oscillators for arbitrary N

In this section, we treat the case of identical oscillators suffering amplitude death for an arbitrary number of globally coupled oscillators, N. For a set of identical oscillators, the frequency distribution of the system is a delta function,

$$g(\omega) = \delta(\omega - \omega_0), \tag{38}$$

where ω_0 is the natural frequency of each oscillator. With this assumption, the matrix B becomes a circulant matrix whose eigenvalues can be expressed in terms of the Nth roots of unity. Since in this particular case only two kinds of coefficients appear in the matrix B, the eigenvalues become much simpler. Explicitly, they are given by

$$\lambda = \left\{1 - K'd + \mathrm{i}\omega_0 + K'd\mathrm{e}^{-\lambda\tau}, 1 - K'd + \mathrm{i}\omega_0 - \frac{K'}{N}\mathrm{e}^{-\lambda\tau}\right\}, \tag{39}$$

in which the second eigenvalue has a degeneracy of $N-1$. Considering both the eigenvalue equations and following a similar procedure as described for the $N = 2$ case, we obtain the following set of critical curves,

$$\tau_{\mathrm{a}}(n, K) = \frac{2n\pi + \cos^{-1}\left[1 - 1/K'd\right]}{\omega_0 - \sqrt{2K'd - 1}}, \tag{40}$$

$$\tau_{\mathrm{b}}(n, K) = \frac{2(n+1)\pi - \cos^{-1}\left[1 - 1/K'd\right]}{\omega_0 + \sqrt{2K'd - 1}}, \tag{41}$$

$$\tau_{\mathrm{c}}(n, K) = \frac{2(n+1)\pi - \cos^{-1}\left[(1 - K'd)/K'(1-d)\right]}{\omega_0 - \sqrt{[K'(1-d)]^2 - (K'd-1)^2}}, \tag{42}$$

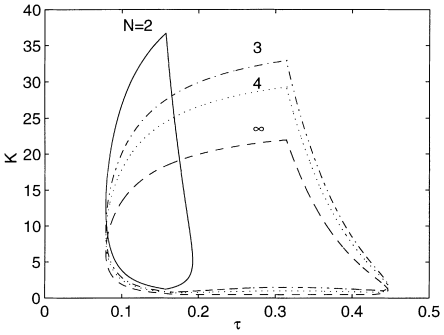

Fig. 9. The existence of death islands for an arbitrary number of globally coupled oscillators. The figure shows the death island regions for $N = 2, 3, 4$ and ∞ plotted from Eqs. (40)–(43) with $n = 0$. All the oscillators are assumed to have an intrinsic frequency of $\omega_0 = 10$. The death island survives even in the limit of $N \to \infty$.

$$\tau_{\mathrm{d}}(n, K) = \frac{2n\pi + \cos^{-1}\left[(1 - K'd)/K'(1 - d)\right]}{\omega_0 + \sqrt{[K'(1 - d)]^2 - (K'd - 1)^2}}. \tag{43}$$

Note that N enters as a parameter (through $d = 1 - 1/N$) in these sets of curves and the family of curves is now four instead of the two found for the $N = 2$ case. In fact for $N = 2$, the curves $\tau_{\mathrm{a}}(n, K)$ and $\tau_{\mathrm{c}}(n, K)$ combine to give $\tau_1(n, K)$ and $\tau_{\mathrm{b}}(n, K)$ and $\tau_{\mathrm{d}}(n, K)$ combine to give $\tau_2(n, K)$ of the previous section. In Fig. 9, we display some typical death island regions for various values of N as obtained from the critical curves (40)–(43) with $n = 0$. The sizes of the islands are seen to vary as a function of N and approach a saturated size as $N \to \infty$. The existence of these regions independently confirmed by direct numerical solution of the coupled oscillator equations, demonstrates that the amplitude death phenomenon for identical oscillators happens even in the case of an arbitrarily large number of oscillators. They also display multiple connectedness of the death region for higher values of ω_0, as was seen for the $N = 2$ case.

3.3. Oscillator death in the thermodynamic limit

In the thermodynamic limit ($N \to \infty, d \to 0$), the summation in the discrete spectrum of Eq. (37) can be replaced by an integral and replacing μ by its definition, the discrete eigenvalue equation can be written as

$$h(\lambda) = \int_{-\infty}^{\infty} \frac{g(\omega)}{\lambda + K' - 1 - \mathrm{i}\omega}\,\mathrm{d}\omega = \frac{1}{K'}\mathrm{e}^{\lambda\tau}, \tag{44}$$

where $g(\omega)$ denotes the distribution of the frequencies. The continuous spectrum is given by

$$\lambda = 1 - K' + \mathrm{i}\omega \quad \text{where} \quad \omega \in g(\omega). \tag{45}$$

From Eq. (45), one can see that one of the critical curves is $K' = 1$. And the amplitude death region should lie to the right of this region in order for the eigenvalues to have negative real parts. To determine the critical curves from the discrete spectrum at $\alpha = 0$, we substitute $\alpha + \mathrm{i}\beta$ for λ in Eq. (44), rationalize the denominator and equate the real and imaginary parts to zero and we have

$$I_1 = \int_{-\infty}^{\infty} \frac{K' - 1}{(K' - 1)^2 + (\beta - \omega)^2} g(\omega)\,\mathrm{d}\omega = \frac{1}{K'}\cos(\beta\tau), \tag{46}$$

$$I_2 = \int_{-\infty}^{\infty} \frac{\omega - \beta}{(K' - 1)^2 + (\beta - \omega)^2} g(\omega)\,\mathrm{d}\omega = \frac{1}{K'}\sin(\beta\tau). \tag{47}$$

These two relations define the other critical curve and for a given $g(\omega)$, they provide a complete analytic description. As an example, let us choose a simple uniform distribution given by

$$g(\omega) = \begin{cases} 1/2\sigma, & \text{if } \omega \in [-\sigma, \sigma], \\ 0, & \text{otherwise.} \end{cases} \tag{48}$$

The integrals I_1 and I_2 can now be explicitly carried out and we get

$$\tan^{-1}\left(\frac{\sigma+\beta}{K'-1}\right) + \tan^{-1}\left(\frac{\sigma-\beta}{K'-1}\right) = \tan^{-1}\left(\frac{2\sigma(K'-1)}{(K'-1)^2-\sigma^2+\beta^2}\right) = \frac{2\sigma}{K'}\cos(\beta\tau), \tag{49}$$

and

$$\log\left(\frac{(K'-1)^2+(\sigma-\beta)^2}{(K'-1)^2+(\sigma+\beta)^2}\right) = \frac{4\sigma}{K'}\sin(\beta\tau). \tag{50}$$

Thus, in the limit of an infinite number of oscillators, the above set of transcendental equations, parametrized by the time delay, provide a complete description of the critical curve for amplitude death (along with $K' = 1$). It is also easy to see that for $\tau = 0$, $\beta = 0$ is the solution one obtains from Eq. (50) and upon substitution of this in Eq. (49), one obtains

$$\tan^{-1}\left(\frac{\sigma}{K'-1}\right) = \frac{\sigma}{K'}, \tag{51}$$

which is the equation for the critical curves in the no delay case as was obtained by [27,28]. In Fig. 10, we plot the region of amplitude death for a typical value of τ. We also note that the general nature of the bifurcation curves is similar to the $N = 2$ case including the occurrence of amplitude death for $\Delta = 0$.

As mentioned earlier, Mirollo and Strogatz [28] also point out that the infinite system provides a fairly accurate description of the large finite system. In order to check this out for the time delayed system, we have carried out numerical studies of a large system ($N = 800$) of oscillators for a few values of K and Δ at a fixed value of τ. The

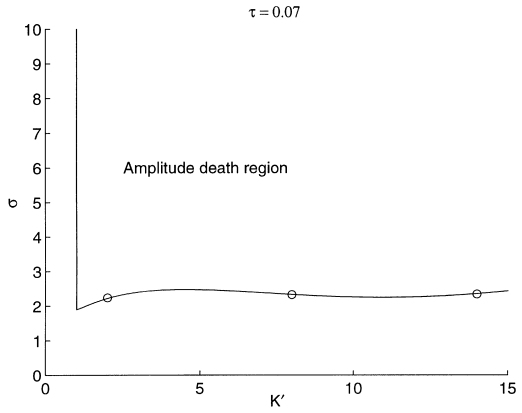

Fig. 10. The amplitude death region for N globally coupled oscillators, as $N \to \infty$ for uniform intrinsic distribution of frequencies, $g(\omega)$, with the average frequency, $\bar{\omega} = 10$ plotted from Eqs. (49) and (50) by eliminating β for $\tau = 0.07$. The death region is bounded by $K' = 1$ and $\tan(\sigma/K') = \sigma/(K'-1)$ for $\tau = 0$. Both the curves meet at a degenerate point $(K', \sigma) = (1, \pi/2)$. As the delay parameter τ is increased, the boundary $K' = 1$ (i.e. $K = 0.5$) still continues to be one of the boundaries. But the second curve distorts in a continuous fashion and at a certain value of τ, it touches the $\sigma = 0$ axis, showing the death of identical oscillators. The points marked, indicate the numerically found value of the boundary for $N = 800$.

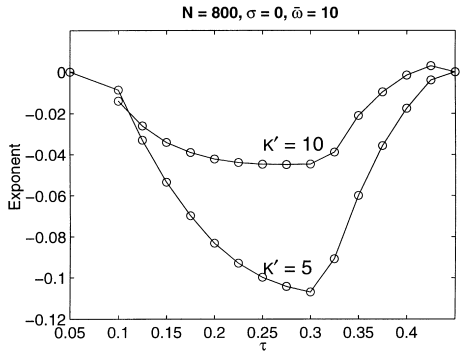

Fig. 11. The rate of approach to the origin of the amplitude of the order parameter, R. If we assume that $R \propto e^{\eta(\tau)t}$, the exponent $\eta(\tau)$ plotted in the above graph shows that the rate of approach to the origin is maximum in the middle of the death island. As one approaches the boundaries of the island on either side, the rate decreases to 0.

values of Δ and K at which the transition from the phase locked region to the death occurs are marked with circles in Fig. 10. As we see these points lie near the analytic curves for the $N = \infty$ case and thus the bifurcation diagram for the finite large system can be expected to be similar to the infinite case.

3.4. Behavior of the order parameter

It is also interesting to examine the behavior of the order parameter in the limit of large number of oscillators, since it provides a good description of the macroscopic behavior of the system. Our particular interest now is to detect any signatures of the time delay effect that might show up in the temporal behavior of the order parameter.

We begin by studying its characteristic behavior in the amplitude death region where it is known to spiral in time to the origin. To investigate the influence of the time delay, we can measure this exponential decay rate for various values of τ. Our numerical results are plotted in Fig. 11 where the decay exponent is plotted against τ for two values of K and for a particular value of ω for the case of $N = 800$ oscillators. The range of τ spans the width of a death island. The exponent is seen to have a maximum negative value in the center of the island and it gets less negative as one moves towards the boundaries. Thus, time delay has a dynamical influence on the rate at which the oscillators collapse into the origin with the maximum rate of decay occurring in the center of the island.

The death islands are surrounded by the phase locked regions in which the order parameter assumes a nonzero constant value. The magnitude of this value is found to be a function of τ. Our numerical results show that the saturated value of the order parameter grows in an algebraic fashion as a function of τ, as we move from the death island boundary into the phase locked region. This is demonstrated in Fig. 12 for $K' = 5$.

Finally, we examine the behavior of the order parameter in the narrow region straddling the boundary between the phase locked and the phase drift region where Matthews and Strogatz [30,31] have found nonstationary behavior corresponding to Hopf oscillations, large oscillations, quasi-periodicity and chaos. We find that the order parameter displays all these characteristic behaviors even in the presence of the time delay. However, there is an overall reduction of the phase space area of this region compared to the no delay case. To see this clearly, we choose to consider the temporal record of the amplitude of the order parameter. The value of the order parameter is constant in the phase locked region, and tends to zero as $1/\sqrt{N}$ with N, the number of the oscillators, in the incoherent region. In the irregular region, a variety of behaviours can be seen. We take a long time record of R discarding the first few hundred points. The average value of this record, $\langle R \rangle$, as shown in Fig. 13, for $N = 500$, shows a plateau

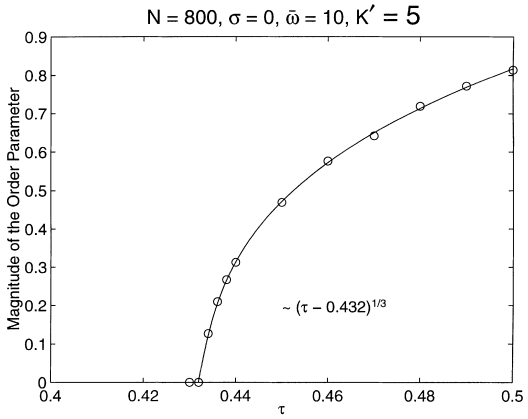

Fig. 12. Power law behavior of the magnitude of the order parameter at the boundary of the death island. The order parameter is 0 inside the death island region due to the fact that the amplitudes of all the oscillators are zero. The order parameter shows a power law behavior at the transition between the death island and the phase locked region. The curve is approximated numerically, at $K' = 5$, by $\tau = 0.432 + 0.0992(R^3 + 0.022R^2 + 0.154R)$.

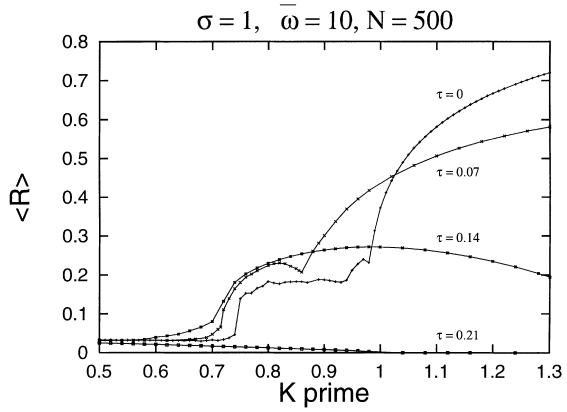

Fig. 13. The effect of the time delay, τ, on the irregular region which was found for $\tau = 0$ by Matthews and Strogatz [30,31]. This region which appears as a plateau for $\tau = 0$, as a whole shrinks as τ is increased. The order parameter is unstable in this region. However, a long temporal record of R gives nearly constant average value. The average value distinguishes the three distinct regions quite accurately. To the right of this plateau region is the phase locked region, and to the left is the incoherent region.

in the irregular region. This is almost unchanged when the number of oscillators is increased from $N = 500$ to $N = 5000$. This region shrinks considerably as the delay parameter τ is increased. We have also observed other qualitative changes in the nature of the time variation of the order parameter which suggest subtle influences of time delay on the dynamical pattern of the nonstationary states. A more detailed and quantitative study of these effects are in progress and will be reported elsewhere.

4. Summary and discussion

We have studied the effect of time delay on the collective dynamics of a system of coupled limit cycle oscillators that are close to a supercritical Hopf bifurcation. The oscillators are linearly coupled in a global fashion and time

delay is introduced in the coupling term. The principal effects of time delay on the stationary collective states like amplitude death and phase locking are clearly evidenced even in a simple two coupled oscillator system. The phase diagram shown in Fig. 7 summarizes these results. The boundary curve for the amplitude death region is a sensitive function of the time delay parameter and the phase space distribution of locked states, amplitude death and incoherent states is quite complex. The phase locked region shows the existence of multiple locked states all of which are stable. A surprising result is the occurrence of amplitude death even for two identical oscillators over a range of time delay values (Fig. 5). Such death islands in the parametric space of the coupling strength and the time delay factor are found to persist even for a large number of identical oscillators. Our numerical findings are backed by analytic results of linear stability of the amplitude death and phase locked states for the $N = 2$ and the $N \to \infty$ cases. The large N results are found to agree very closely with the $N \to \infty$ curves. For the case of identical oscillators, we provide exact analytic curves for the island boundaries. Our principal focus has been on the investigation of the stationary states but we have also confirmed the existence of the nonstationary states (e.g. Hopf oscillations, chaos etc.) in the finite time delay model. We hope to carry out a more detailed investigation of these states in the future.

As we have mentioned earlier, time delay effects in the context of the coupled oscillator model have not been looked at before. In view of the vast number of applications of the coupled oscillator model, our results may have significance for some biological or physical systems. There are many physical examples of amplitude death in real systems. One of the earliest that was investigated both theoretically and experimentally is that of coupled chemical oscillator systems e.g. coupled Belousov–Zhabotinskii reactions carried out in coupled stirred tank reactors [12,29]. They can also occur in ecological contexts where one can imagine two sites each having the same predator–prey mechanism which causes the number density of the species to oscillate. If the species are capable of moving from site to site at a proper rate (appropriate coupling strength), the two sites may become stable (stop oscillating) and acquire constant populations. Another important application of this concept is in pathologies of biological oscillator networks e.g. an assembly of cardiac pacemaker cells [15,16]. Amplitude death signifies cessation of rhythmicity in such a system which is normally, spontaneously rhythmic for other choices of parameters. For the onset of such an arrhythmia, current models based on Coupled oscillator networks need to assume a significant spread in the natural frequencies of the constituent cells (oscillators) [28]. Our result of amplitude death demonstrates that this assumption may not be necessary if one takes into account, time delay effects arising naturally from the finite propagation times of the signals exchanged between the cells. Another possible application is in the area of high power microwave sources where it is proposed to enhance the microwave power production by phase locking a large number of sources such as relativistic magnetrons [9]. Time delay effects, arising from the finite propagation time of information signals traveling through the connecting waveguide bridges, could impose important limitations on the connector lengths and geometries in these schemes. Our findings could provide a guideline in this direction. Coupled oscillators featuring in several neural network configuration where multiple phase locked states arising from time delay effects, could play an important role.

Finally, we would like to discuss some further extensions of the present work and possible future directions of research in this area. Our present results have been largely derived from the simple model of limit cycle oscillators, which are close to a supercritical Hopf bifurcation and which are linearly coupled in a global fashion. It would be interesting to carry out a similar analysis for limit cycle oscillators with local coupling. For the particular case of death of identical oscillators, we have confirmed that the result holds for the locally coupled model as well, but a more general investigation of other collective states remains to be done. Likewise, the introduction of more complicated dynamics in the individual oscillators, such as shear (amplitude dependent frequency) [24] and higher order nonlinearities can open up rich possibilities for the interplay of time delay and the collective dynamics of the system.

Appendix A. Stability of the frequency locked solutions

The phase locked solutions for the case of $N = 2$ are given by $(\psi_1, \psi_2, \psi_3, \psi_4) = (R_1, R_2, \Omega t - \alpha/2, \Omega t + \alpha/2)$. To determine the stability of the phase locked states, we carry out a linear perturbation analysis about these solutions. Suppose λ represents the eigenvalue, the characteristic equation is then given by

$$\det \begin{vmatrix} A-\lambda & C_1 e^{-\lambda\tau} & R_2 D_1 & -R_2 D_1 e^{-\lambda\tau} \\ C_2 e^{-\lambda\tau} & B-\lambda & -R_1 D_2 e^{-\lambda\tau} & R_1 D_2 \\ -\frac{R_2}{R_1^2} D_1 & \frac{D_1}{R_1} e^{-\lambda\tau} & \frac{-R_2}{R_1} C_2 - \lambda & \frac{R_2}{R_1} C_1 e^{-\lambda\tau} \\ \frac{D_2}{R_2} e^{-\lambda\tau} & -\frac{R_1}{R_2^2} D_2 & \frac{R_1}{R_2} C_2 e^{-\lambda\tau} & -\frac{R_1}{R_2} C_1 - \lambda \end{vmatrix} = 0, \tag{A.1}$$

where $A = 1 - K - 3R_1^2$, $B = 1 - K - 3R_2^2$, $C_1 = K\cos(-\Omega\tau + \alpha)$, $C_2 = K\cos(\Omega\tau + \alpha)$, $D_1 = K\sin(-\Omega\tau + \alpha)$, $D_2 = K\cos(-\Omega\tau - \alpha)$. We can also write the above determinant in the form of the following equation,

$$f_{00} + f_{01}\lambda + f_{02}\lambda^2 + f_{04}\lambda^4 + (f_{20} + f_{21}\lambda + f_{22}\lambda^2)e^{-2\lambda\tau} + f_4 e^{-4\lambda\tau} = 0, \tag{A.2}$$

where the coefficient functions f_{ij} are given by

$$f_{00} = ABC_1C_2 + D_1^2D_2^2 - \frac{AC_2D_2^2R_1}{R_2} - \frac{BC_1D_1^2R_2}{R_1}, \tag{A.3}$$

$$f_{01} = -AC_1C_2 - BC_1C_2 - \frac{AD_2^2R_1^2}{R_2^2} - \frac{BD_1^2R_2^2}{R_1^2} + \frac{ABC_1R_1}{R_2} + \frac{ABC_2R_2}{R_1} + \frac{C_2D_2^2R_1}{R_2} + \frac{C_1D_1^2R_2}{R_1}, \tag{A.4}$$

$$f_{02} = AB + C_1C_2 + \frac{D_1^2R_2^2}{R_1^2} + \frac{D_2^2R_1^2}{R_2^2} - \frac{AC_1R_1}{R_2} - \frac{BC_1R_1}{R_2} - \frac{AC_2R_2}{R_1} - \frac{BC_2R_2}{R_1}, \tag{A.5}$$

$$f_{04} = -A - B + \frac{C_1R_1}{R_2} + \frac{C_2R_2}{R_1}, \tag{A.6}$$

$$f_{20} = -ABC_1C_2 - C_1^2C_2^2 - C_1C_2D_1^2 - C_1C_2D_2^2 - C_1^2D_1D_2 - C_2^2D_1D_2 + 2C_1C_2D_1D_2 - 2D_1^2D_2^2 - \frac{AC_1D_1D_2R_1}{R_2} + \frac{AC_2D_1D_2R_1}{R_2} + \frac{BC_1D_1D_2R_2}{R_1} - \frac{BC_2D_1D_2R_2}{R_1} + \frac{AC_1D_2^2R_1}{R_2} + \frac{BC_2D_1^2R_2}{R_1}, \tag{A.7}$$

$$f_{21} = AC_1C_2 + BC_1C_2 - AD_1D_2 - BD_1D_2 - \frac{C_1^2C_2R_1}{R_2} - \frac{C_1C_2^2R_2}{R_1} + \frac{C_1D_1D_2R_1}{R_2} + \frac{C_2D_1D_2R_2}{R_1} - \frac{2C_2D_1D_2R_1}{R_2} - \frac{2C_1D_2^2R_1}{R_2} - \frac{2C_2D_1^2R_2}{R_1} - \frac{2C_1D_1D_2R_2}{R_1}, \tag{A.8}$$

$$f_{22} = -2C_1C_2 + 2D_1D_2, \tag{A.9}$$

$$f_4 = C_1^2C_2^2 + C_2^2D_1^2 + C_1^2D_2^2 + D_1^2D_2^2 = 1. \tag{A.10}$$

Eq. (A.2) has been solved numerically to generate the stability curves displayed in the paper.

References

[1] A.A. Brailove, P.S. Linsay, An experimental study of a population of relaxation oscillators with a phase-repelling mean-field coupling, Int. J. Bifurcation Chaos 6 (1996) 1211.
[2] K. Satoh, Computer experiments on the co-operative behavior of a network of interacting nonlinear oscillators, J. Phys. Soc. Jpn. 58 (1989) 2010.
[3] P. Hadley, M.R. Beasley, K. Wiesenfeld, Phase locking of Josephson-junction series arrays, Phys. Rev. B 38 (1988) 8712.
[4] P. Hadley, M.R. Beasley, K. Wiesenfeld, Phase locking of Josephson-junction arrays, Appl. Phys. Lett. 52 (1988) 1619.
[5] K. Wiesenfeld, P. Colet, S.H. Strogatz, Synchronization transitions in a disordered Josephson series array, Phys. Rev. Lett. 76 (1996) 404.
[6] P.M. Varangis, A. Gavrielides, T. Erneux, V. Kovanis, L.F. Lester, Frequency entrainment in optically injected semiconductor lasers, Phys. Rev. Lett. 78 (1997) 2353.
[7] A. Hohl, A. Gavrielides, T. Erneux, V. Kovanis, Localized synchronization in two coupled nonidentical semiconductor lasers, Phys. Rev. Lett. 78 (1997) 4745.
[8] G. Grüner, A. Zettl, Charge density wave conduction: a novel collective transport phenomenon in solids, Phys. Rep. 119 (1985) 117.
[9] J. Benford, H. Sze, W. Woo, R.R. Smith, B. Harteneck, Phase locking of relativistic magnetrons, Phys. Rev. Lett. 62 (1989) 969.
[10] I. Schreiber, M. Marek, Strange attractors in coupled reaction diffusion cells, Physica D 5 (1982) 258.
[11] Y. Kuramoto, Chemical Oscillations, Waves and Turbulence, Springer, Berlin, 1984.
[12] M.F. Crowley, I.R. Epstein, Experimental and theoretical studies of a coupled chemical oscillator: phase death, multistability, and in-phase and out-of-phase entrainment, J. Phys. Chem. 93 (1989) 2496.
[13] M. Dolnik, I.R. Epstein, Coupled chaotic chemical oscillators, Phys. Rev. E 54 (1996) 3361.
[14] M. Kawato, R. Suzuki, Two coupled neural oscillators as a model of the circadian pacemaker, J. Theor. Biol. 86 (1980) 547.
[15] A.T. Winfree, The Geometry of Biological Time, Springer, New York, 1980.
[16] A.T. Winfree, The Three-Dimensional Dynamics of Electrochemical Waves and Cardiac Arrythmias, Princeton University Press, Princeton, NJ, 1987.
[17] Y. Kuramoto, Co-operative dynamics of oscillator community, Prog. Theor. Phys. Suppl. 79 (1984) 223.
[18] Y. Kuramoto, I. Nishikawa, Statistical macrodynamics of large dynamical systems: case of a phase transition in oscillator communities, J. Stat. Phys. 49 (1987) 569.
[19] H. Daido, Intrinsic fluctuations and a phase transition in a class of large populations of interacting oscillators, J. Stat. Phys. 60 (1990) 753.
[20] H. Daido, Multibranch entrainment and scaling in large populations of coupled oscillators, Phys. Rev. Lett. 77 (1996) 1406.
[21] H. Daido, Onset of co-operative entrainment in limit-cycle oscillators with uniform all-to-all interactions: bifurcation of the order function, Physica D 91 (1996) 24.
[22] Y. Aizawa, Synergetic approach to the phenomena of mode-locking in nonlinear systems, Prog. Theor. Phys. 56 (1976) 703.
[23] M. Shiino, M. Frankowicz, Synchronization of infinitely many coupled limit-cycle oscillators, Phys. Lett. A 136 (1989) 103.
[24] M. Poliashenko, S.R. McKay, Chaos due to homoclinic orbits in two coupled oscillators with nonisochronism, Phys. Rev. A 46 (1992) 5271.
[25] J.L. Rogers, L.T. Wille, Phase transitions in nonlinear oscillator chains, Phys. Rev. E 54 (1996) R2193.
[26] D.G. Aronson, G.B. Ermentrout, N. Koppel, Amplitude response of coupled oscillators, Physica D 41 (1990) 403.
[27] G.B. Ermentrout, Oscillator death in populations of 'all to all' coupled nonlinear oscillators, Physica D 41 (1990) 219.
[28] R.E. Mirollo, S.H. Strogatz, Amplitude death in an array of limit-cycle oscillators, J. Stat. Phys. 60 (1990) 245.
[29] K. Bar-Eli, On the stability of coupled chemical oscillators, Physica D 14 (1985) 242.
[30] P.C. Matthews, S.H. Strogatz, Phase diagram for the collective behavior of limit-cycle oscillators, Phys. Rev. Lett. 65 (1990) 1701.
[31] P.C. Matthews, R.E. Mirollo, S.H. Strogatz, Dynamics of a large system of coupled nonlinear oscillators, Physica D 52 (1991) 293.
[32] R. Vallée, P. Dubois, M. Côté, C. Delisle, Second-order differential-delay equation to describe a hybrid bistable device, Phys. Rev. A 36 (1987) 1327.
[33] N. Minorsky, Self-excited mechanical oscillations, J. Appl. Phys. 19 (1948) 332.
[34] J. Faro, S. Velasco, An approximation for prey–predator models with time delay, Physica D 110 (1997) 313.
[35] U. Ernst, K. Pawelzik, T. Geisel, Synchronization induced by temporal delays in pulse-coupled oscillators, Phys. Rev. Lett. 74 (1995) 1570.
[36] S.R. Campbell, D. Wang, Relaxation oscillators with time delay coupling, Physica D 111 (1998) 151.
[37] H.G. Schuster, P. Wagner, Mutual entrainment of two limit-cycle oscillators with time delayed coupling, Prog. Theor. Phys. 81 (1989) 939.
[38] E. Niebur, H.G. Schuster, D. Kammen, Collective frequencies and metastability in networks of limits-cycle oscillators with time delay, Phys. Rev. Lett. 67 (1991) 2753.
[39] Y. Nakamura, F. Tominaga, T. Munakata, Clustering behavior of time-delayed nearest-neighbor coupled oscillators, Phys. Rev. E 49 (1994) 4849.
[40] S. Kim, S.H. Park, C.S. Ryu, Multistability in coupled oscillator systems with time delay, Phys. Rev. Lett. 79 (1997) 2911.
[41] D.V.R. Reddy, A. Sen, G.L. Johnston, Time delay induced death in coupled limit cycle oscillators, Phys. Rev. Lett. 80 (1998) 5109.